Quantum-to-classical correspondence in two-dimensional Heisenberg models

Tao Wang 0, 1 Xiansheng Cai, 1 Kun Chen, 2 Nikolay V. Prokof'ev, 1,3 and Boris V. Svistunov 1,3,4 ¹Department of Physics, University of Massachusetts, Amherst, Mafssachusetts 01003, USA ²Department of Physics and Astronomy, Rutgers University, Piscataway, New Jersey 08854, USA ³National Research Center "Kurchatov Institute," 123182 Moscow, Russia ⁴Wilczek Quantum Center, School of Physics and Astronomy, Shanghai Jiao Tong University, Shanghai 200240, China

(Received 29 April 2019; revised manuscript received 30 September 2019; published 17 January 2020)

The quantum-to-classical correspondence (QCC) in spin models is a puzzling phenomenon where the static susceptibility of a quantum system agrees with its classical-system counterpart, at a different corresponding temperature, within the systematic error at a subpercent level. We employ the bold diagrammatic Monte Carlo method to explore the universality of QCC by considering three different two-dimensional spin-1/2 Heisenberg models. In particular, we reveal the existence of QCC in models with two parameters.

DOI: 10.1103/PhysRevB.101.035132

I. INTRODUCTION

The quantum-to-classical correspondence (QCC) is a recently discovered phenomenon where the static susceptibility of a certain spin model (at any available temperature T_O and lattice distance r) can be accurately reproduced, up to a global normalization factor, by its classical counterpart at the corresponding temperature T_C . The QCC was first revealed by Kulagin et al. [1] for the square- and triangular-lattice spin-1/2 Heisenberg antiferromagnets [1]. QCC was subsequently established for the pyrochlore lattice Heisenberg antiferromagnet [2]. Up to now, the origin of QCC still remains unknown, which motivates us to further study the universal applicability of QCC in two-dimensional (2D) spin systems.

In this article, we verify the existence of the QCC for three 2D frustrated magnets: the kagome-lattice Heisenberg antiferromagnet (KLHA), the square-lattice $J_1 - J_2$ model, and the spatially anisotropic triangular-lattice Heisenberg antiferromagnet (ATLHA), all of which are of great experimental and numerical interest [3–5]. All considered Hamiltonians can be described as

$$H = \sum_{\langle ij\rangle} J_{ij} \, \mathbf{S}_i \cdot \mathbf{S}_j \;, \tag{1}$$

where $\langle ij \rangle$ stands for all pairs of interacting lattice sites as illustrated for each model in Fig. 1, and J_{ij} are the corresponding coupling constants. For KLHA, $J_{ij} = J$, while for the other two models J_{ij} can take two different values, J_1 and J_2 . The only difference between the quantum and classical models is that spin-1/2 operators **S** are replaced with unit vectors.

It is worth noting that the QCC only applies to the static susceptibility expressed by the correlator

$$\chi(\mathbf{r}) \equiv \int_0^\beta d\tau \, \chi(\mathbf{r}, \tau) = \int_0^\beta d\tau \, \langle \mathbf{S}(0, 0) \cdot \mathbf{S}(\mathbf{r}, \tau) \rangle \,, \quad (2)$$

where $S(\mathbf{r}, \tau)$ is the Matsubara spin-1/2 operator. The equaltime correlation function, $\chi(\mathbf{r}, \tau = 0)$, while having a qualitatively similar spatial profile, does not match the classical correlation function. It is thus surprising to observe that the static quantum and classical correlations, despite featuring a highly nontrivial and model-dependent pattern of sign-alternating spatial fluctuations, demonstrate perfect qualitative and extremely accurate quantitative agreement (see Figs. 2 and 3).

On the one hand, it is believed that the quantum KLHA is one of the most promising candidates for a spin liquid ground state that does not break the spin-rotation and latticetranslation symmetries [6–9]. On the other hand, it has been reported that the classical KLHA is located at a tricritical point where three different ordered states coexist [10]. The proposed quantum and classical ground states are, thus, dramatically different, which apparently denies the existence of QCC at least at low enough temperature. We verify that the QCC remains valid at temperatures $T/J \ge 1/3$. Unfortunately, limitations of the bold diagrammatic Monte Carlo method (BDMC) based on the G^2W expansion [1] do not allow us to access lower temperatures to ensure that the ground-state properties are dominating in the correlation function [11]. Whether QCC is valid at much lower temperature remains to be seen in the future.

The square-lattice $J_1 - J_2$ model enables us to explicitly check the validity of QCC in the different phases of the same system. Numerous previous works have established the rich ground-state phase diagram of this model with respect to changing the J_2/J_1 ratio [4]. Apart from the spin liquid state predicted for $0.41 \le J_2/J_1 \le 0.62$ [12], it also features three ordered states: ferromagnetic (FM), Néel antiferromagnetic (NAF), and collinear antiferromagnetic (CAF). We choose the following parameter sets in this work: $(J_1 = 1.0, J_2 = 0.5)$ to address the mostly frustrated case and $(J_1 = -1.0, J_2 = 0.4)$ in the CAF phase (notice the ferromagnetic sign of the nearest neighbor interaction). Here and in what follows, we choose the modulus of J_1 as the unit of energy.

The ATLHA model is chosen specifically to study how moderate anisotropy in the coupling constants effects the QCC. In this case, we choose $J_2/J_1 = 0.33$, which is the same as the ratio used to explain experimental data in Cs₂CuCl₄ [5]. When the anisotropy is very strong, the ATLHA model resembles decoupled one-dimensional (1D) chains, for which

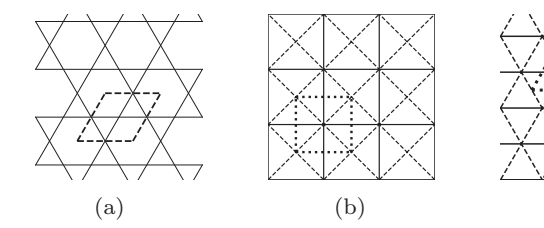


FIG. 1. Specifying interactions and primitive cells for three spin models: (a) kagome-lattice model, (b) square-lattice J_1-J_2 model, and (c) anistropic triangular-lattice model. In panel (a), all bonds have the same coupling constant J. In panels (b) and (c), solid and dashed lines represent coupling constants J_1 and J_2 respectively, while dotted lines define the primitive cells.

(c)

the QCC does not hold [1]. It appears that observing the crossover between the 1D and 2D behavior requires very small ratios of the coupling constants, and the fascinating QCC phenomenon is robust against anisotropy.

To obtain the static spin-spin correlation function for quantum models, we employ the BDMC method that allows one to study any frustrated spin model in the cooperative paramagnetic regime at temperatures below the exchange coupling constant J [1,2]. The relative accuracy of the converged BDMC results is $\approx 1\%$ (the loss of convergence is the prime reason preventing the method from being used at very low temperature). All models were simulated on lattices with periodic boundary conditions and system sizes $L \times L = 16 \times 16$ in terms of primitive cells. These system sizes are much larger than the correlation length to ensure that finite-size corrections to presented results are negligible (the correlation functions decrease by about four orders of magnitude before reaching distances L/4 along the primitive cell directions). The primitive cells and sample geometry are showed in Fig. 1.

Establishing QCC for single-parameter models boils down to one-to-one correspondence between the temperatures of quantum, T_Q , and classical, T_C , systems, for which the difference between the normalized correlation functions, $\chi(r)/\chi(0)$, is minimized. This "one-dimensional" T_Q -to- T_C mapping applies to KLHA. More interesting results are obtained for the other two models, both of which feature an

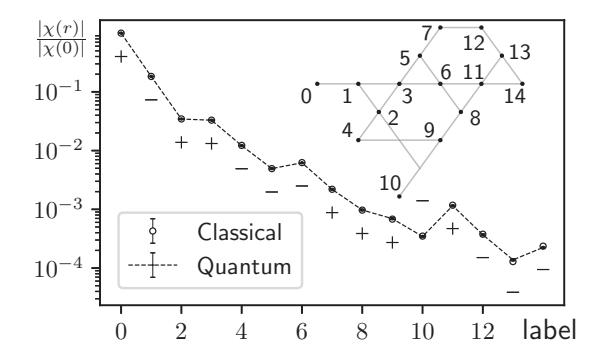


FIG. 2. Accurate (within the accuracy bounds) match between the normalized quantum (dots connected by the dashed line) and classical (open circles) correlation functions of the kagome-lattice Heisenberg antiferromagnet at $T_Q=1.0$. The sequence of labeled distances is illustrated in the top right corner. The sign of the correlation function is indicated explicitly next to each point.

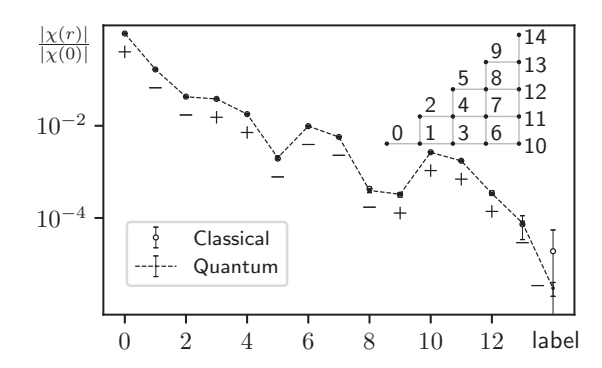


FIG. 3. Accurate match of the normalized static quantum (dots connected by the dashed line) and classical (open circles) correlation functions for the square-lattice $J_1 - J_2$ model at $T_Q = 1.0$. The sequence of labeled distances is illustrated in the top right corner. The sign of the correlation function is indicated explicitly next to each point.

additional model parameter J_2 . It turns out that not only the temperature but also J_2 need to be fine-tuned to obtain the best match between the quantum and classical correlation functions if we choose to stay in the same model subspace. To be more specific, we find that for the quantum model with $J_2^Q \neq 0$ at temperature T_Q , the matching classical counterpart should be taken with $J_2^C \neq J_2^Q$ at temperature T_C (asymptotically, $J_2^C \to J_2^Q$ at high temperature). This constitutes a "two-dimensional" (T_Q, J_2^Q) - (T_C, J_2^C) mapping.

In what follows, we establish that at all accessible temperatures all models demonstrate a perfect (within error bars) match between the static quantum and classical correlation functions. We discuss properties of the correspondence mapping and conclude with broader implications of this work, as well as perspectives for future developments.

II. RESULTS

The precise protocol for establishing the QCC is as follows. We first compute the static correlation function of the quantum system by the BDMC method. The answer for its classical counterpart $\chi_C(\mathbf{r})$ was obtained by the conventional single-spin flip Monte Carlo method. Next, we normalize the quantum result to unity at the origin $[\chi_C(\mathbf{r}=0)=1]$ automatically, to obtain $f(\mathbf{r})=\chi(\mathbf{r})/\chi(0)$. Finally, we fine-tune classical system parameters—which are, in our case, T_C/J_1 and J_2^C —to find the best fit to the $f(\mathbf{r})$ curves. We repeat this process at different temperatures T_Q or values of J_2^Q , to obtain the correspondence curves.

Note that we have only one or two fitting parameters to describe the entire functional dependence of f on distance, including numerous, and often irregular, sign changes and an order of magnitude strong fluctuations. Remarkably, all these features can be reproduced by the classical model at all distances within the error bounds of our calculations (often at the subpercent level for several closets sites). In Figs. 2 and 3, we show examples of QCC for KLHA and the square-lattice $J_1 - J_2$ model at $T_Q = 1.0$. Absolute values of all results shown in both plots are also presented in Tables I and II because for most data points the error bars are

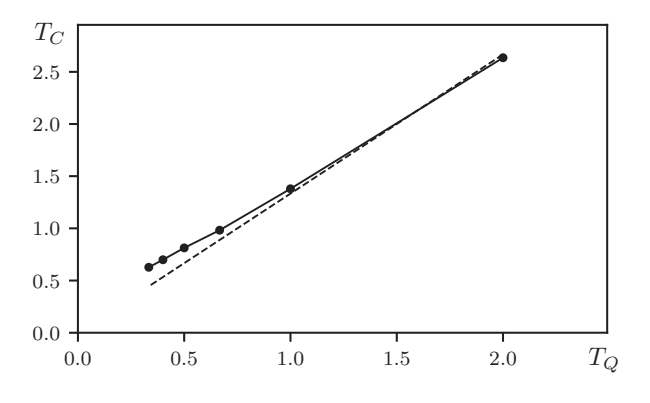
TABLE I. Absolute values of quantum and classical correlation functions of kagome-lattice model presented in Figs. 2, along with the error bounds on the difference between the two. The error bounds are based on the 3σ -criterion for purely statistical Monte Carlo fluctuations and the systematic error of the extrapolation to the infinite diagram order limit for quantum simulations. Accurate QCC is observed for all points within the error bounds.

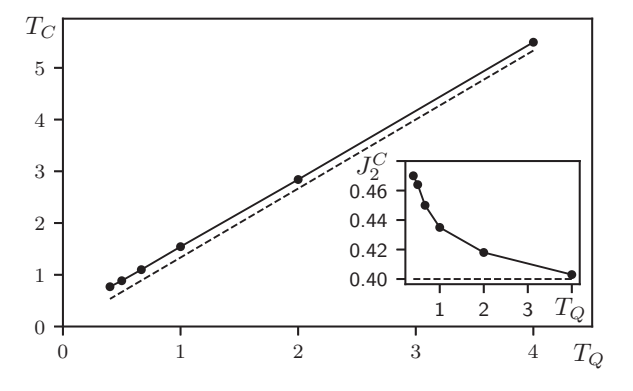
Space	Classical	Quantum	Correlator	
Label	Correlator	Correlator	Difference	Error bar
0	1.000000	1.000000	0.000000	0.000000
1	0.182995	0.183641	0.000646	0.000978
2	0.034589	0.034820	0.000231	0.000342
3	0.033010	0.033191	0.000181	0.000319
4	0.012270	0.012339	0.000069	0.000148
5	0.004932	0.005005	0.000073	0.000104
6	0.006247	0.006291	0.000044	0.000069
7	0.002195	0.002225	0.000030	0.000052
8	0.000969	0.000994	0.000025	0.000029
9	0.000681	0.000703	0.000022	0.000024
10	0.000350	0.000353	0.000003	0.000013
11	0.001175	0.001174	0.000001	0.000025
12	0.000377	0.000378	0.000001	0.000016
13	0.000129	0.000141	0.000012	0.000012
14	0.000236	0.000229	0.000007	0.000012

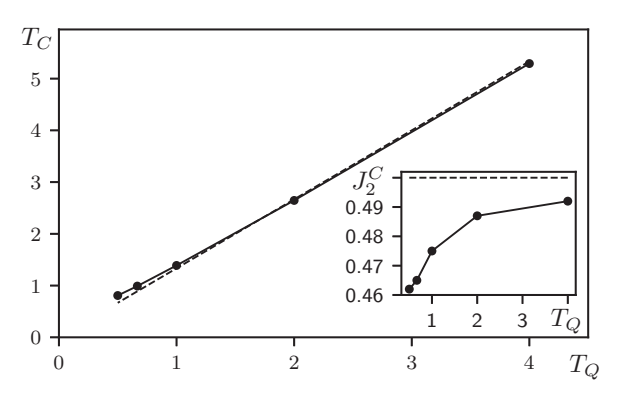
smaller than symbol sizes. We observe that an accurate match can be achieved, and this holds at all temperatures accessible to us and for all models studied in this work. As of now, no exception from the QCC "rule" was found in dimensions d > 1.

TABLE II. Absolute values of quantum and classical correlation functions of square-lattice J1-J2 model presented in Figs. 3, along with the error bounds on the difference between the two. The error bounds are based on the 3σ -criterion for purely statistical Monte Carlo fluctuations and the systematic error of the extrapolation to the infinite diagram order limit for quantum simulations. Accurate QCC is observed for all points within the error bounds.

Space	Classical	Quantum	Correlator	
Label	Correlator	Correlator	Difference	Error bar
0	1.000000	1.000000	0.000000	0.000000
1	0.166453	0.166971	0.000518	0.002629
2	0.042818	0.042386	0.000432	0.000448
3	0.038162	0.038169	0.000007	0.000914
4	0.017860	0.017840	0.000020	0.000219
5	0.001943	0.002026	0.000083	0.000217
6	0.009799	0.009810	0.000011	0.000299
7	0.005713	0.005695	0.000018	0.000140
8	0.000428	0.000394	0.000034	0.000069
9	0.000320	0.000327	0.000007	0.000046
10	0.002663	0.002653	0.000010	0.000123
11	0.001741	0.001731	0.000010	0.000083
12	0.000347	0.000340	0.000007	0.000040
13	0.000073	0.000078	0.000005	0.000046
14	0.000019	0.000003	0.000016	0.000037







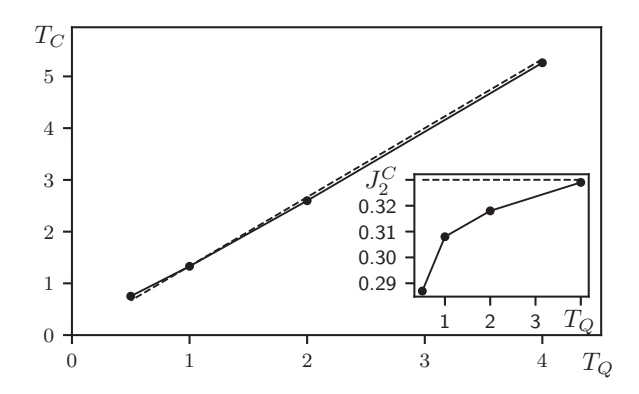


FIG. 4. Correspondence curves of all models. From top to the bottom: KLHA; square-lattice CAF ($J_1=-1.0,\,J_2=0.4$); square-lattice QSL ($J_2/J_1=0.5$); and ATLHA ($J_2/J_1=0.33$). The high-temperature asymptotic relations $T_C=(4/3)T_Q$ and $J_2^C=J_2^Q$ are indicated by the dashed lines.

The free parameters of the classical model, T_C and J_2^C are plotted in Fig. 4 as functions of the quantum model

temperature T_Q , together with the high-temperature asymptotic relations $T_C = (4/3)T_Q$ and $J_2^C = J_2^Q$, which can be easily verified by the high-temperature expansion. The first relation merely reflects the difference between $\langle S^2 \rangle = S(S+1) =$ 3/4 and $\langle \mathbf{n}^2 \rangle = 1$. (For models with two parameters, the QCC represents a 2D mapping. If we keep J_2^Q fixed, we can still present it as the correspondence curves). It is worth noting that J_2^C of the square-lattice $J_1 - J_2$ model approaches J_2^{\emptyset} from different sides when we change the sign of J_1 . Mapping of spin-spin correlation functions between the quantum and classical models is rather standard and expected in two limiting cases. At $T/J \gg 1$, it can be established analytically by looking at the lowest-order high-temperature series expansion contribution capturing the weak short-range correlations. At distances beyond the small correlation length, both systems are described by the universal coarse-grained field statistics. The QCC in the cooperative paramagnetic regime, $T/J \lesssim 1$, is fundamentally different from these limiting cases: On the one hand, correlations at short distance are strong and far from being accurately described by the lowest-order hightemperature series expansion; on the other hand, the correlation length remains short and the coarse-grained description is not applicable.

III. DISCUSSION

Using the BDMC technique, we computed the static spinspin correlations as functions of distance for three different frustrated spin models, including the cooperative paramagnetic regime that, as far as we know, cannot be addressed for large system sizes by any of the other numerical methods. We found that all systems feature the nontrivial quantum-toclassical correspondence. We measured the correspondence curves for each model down to temperatures below the exchange coupling constant and verified that each curve follows the expected asymptotic behavior in the high-temperature limit.

Future numerical work with respect to QCC can follow two different routes. (i) Extend the low-temperature range for quantum systems. Our current implementation of the BDMC technique faces convergence problems at temperature $T \ll J$ and does not allow us to obtain data at sufficiently low T for reliable extrapolation to the ground state. Making predictions based on QCC with regards to the spin liquid ground state is not possible under these conditions. There exist numerous alternative formulations of the diagrammatic expansion [13] and ways of regrouping and resumming diagrammatic series; some of them may prove helpful in extending the range of temperatures where the diagrammatic Monte Carlo technique works. (ii) Expand the "family" of models demonstrating the QCC in dimensions d > 1 or find exceptions from the "rule." Without proper theoretical understanding of its origin, it is worth exploring how other model features, such as long-range coupling, affect QCC.

Other finite-temperature methods [14–16] can, in principle, address the T/J < 1 regime of the 2D Heisenberg models, but they all have important disadvantages when compared with BDMC. Methods based on exact diagonalization are limited to small system sizes; e.g., for KLHA the finite-temperature Lanczos method can only deal with about 40 lattice sites, leaving no space for studies of spatial profiles at distances $r \ll L/2$. Since static susceptibility $\chi(r)$ is not based on the correlation function of conserved quantities—such as energy or uniform magnetization—it is not simulated by high-temperature expansion methods due to prohibiting computational complexity involved. New methods, such as the infinite projected entangled pair states at finite temperature [17], have the potential to change this situation in the future.

ACKNOWLEDGMENTS

This work was supported by the Simons Collaboration on the Many Electron Problem, the National Science Foundation under Grant No. DMR-1720465, and the MURI Program "New Quantum Phases of Matter" from AFOSR.

^[1] S. A. Kulagin, N. Prokof'ev, O. A. Starykh, B. Svistunov, and C. N. Varney, Phys. Rev. Lett. **110**, 070601 (2013).

^[2] Y. Huang, K. Chen, Y. Deng, N. Prokof'ev, and B. Svistunov, Phys. Rev. Lett. 116, 177203 (2016).

^[3] T. Imai, E. A. Nytko, B. M. Bartlett, M. P. Shores, and D. G. Nocera, Phys. Rev. Lett. 100, 077203 (2008).

^[4] O. Mustonen, S. Vasala, K. P. Schmidt, E. Sadrollahi, H. C. Walker, I. Terasaki, F. J. Litterst, E. Baggio-Saitovitch, and M. Karppinen, Phys. Rev. B 98, 064411 (2018).

^[5] R. Coldea, D. A. Tennant, A. M. Tsvelik, and Z. Tylczynski, Phys. Rev. Lett. 86, 1335 (2001).

^[6] S. Sachdev, Phys. Rev. B 45, 12377 (1992).

^[7] S. Yan, D. A. Huse, and S. R. White, Science **332**, 1173 (2011)

^[8] S. Depenbrock, I. P. McCulloch, and U. Schollwöck, Phys. Rev. Lett. 109, 067201 (2012).

^[9] Y. Iqbal, F. Becca, S. Sorella, and D. Poilblanc, Phys. Rev. B 87, 060405(R) (2013).

^[10] L. Messio, B. Bernu, and C. Lhuillier, Phys. Rev. Lett. 108, 207204 (2012).

^[11] T. Shimokawa and H. Kawamura, J. Phys. Soc. Jpn. 85, 113702 (2016).

^[12] H.-C. Jiang, H. Yao, and L. Balents, Phys. Rev. B 86, 024424 (2012).

^[13] R. Rossi, F. Werner, N. Prokof'ev, and B. Svistunov, Phys. Rev. B 93, 161102(R) (2016).

^[14] J. Schnack, J. Schulenburg, and J. Richter, Phys. Rev. B 98, 094423 (2018).

^[15] C. Karrasch, J. H. Bardarson, and J. E. Moore, Phys. Rev. Lett. 108, 227206 (2012).

^[16] N. E. Sherman and R. R. P. Singh, Phys. Rev. B 97, 014423 (2018).

^[17] P. Czarnik and P. Corboz, Phys. Rev. B 99, 245107 (2019).